Check for updates

Received: 7 February 2020 | Revised: 30 April 2020 | Accepted: 4 May 2020

DOI: 10.1111/mec.15466

ORIGINAL ARTICLE

MOLECULAR ECOLOGY WILEY

A ketocarotenoid-based colour polymorphism in the Sira poison frog *Ranitomeya sirensis* indicates novel gene interactions underlying aposematic signal variation

Evan Twomey[1,2] | James D. Johnson[3] | Santiago Castroviejo-Fisher[1,4] | Ines Van Bocxlaer[2]

[1]Laboratorio de Sistemática de Vertebrados, Pontificia Universidade Católica do Rio Grande do Sul (PUCRS), Porto Alegre, Brazil

[2]Amphibian Evolution Laboratory, Biology Department, Vrije Universiteit Brussel, Brussels, Belgium

[3]Department of Chemistry, Florida State University, Tallahassee, FL, USA

[4]Department of Herpetology, American Museum of Natural History, New York, NY, USA

Correspondence
Evan Twomey, Faculty of Biological Sciences, Goethe University Frankfurt, Frankfurt am Main, Germany
Email: evan.twomey@gmail.com

Funding information
Fonds voor Wetenschappelijk Onderzoek, Grant/Award Number: G0D6618N; Coordenação de Aperfeiçoamento de Pessoal de Nível Superior, Grant/Award Number: 88881.067967/2014-01; Strategic Research Programme of the Vrije Universiteit Brussel, Grant/Award Number: SRP30

Abstract

The accumulation of red ketocarotenoids is an important component of coloration in many organisms, but the underlying mechanisms are poorly understood. In some organisms, ketocarotenoids are sequestered from the diet and can accumulate when enzymes responsible for carotenoid breakdown are disrupted. In other organisms, ketocarotenoids are formed endogenously from dietary precursors via oxidation reactions carried out by carotenoid ketolase enzymes. Here, we study the genetic basis of carotenoid coloration in an amphibian. We demonstrate that a red/yellow polymorphism in the dendrobatid poison frog *Ranitomeya sirensis* is due to the presence/absence of ketocarotenoids. Using whole-transcriptome sequencing of skins and livers, we found that a transcript encoding a cytochrome P450 enzyme (CYP3A80) is expressed 3.4-fold higher in livers of red frogs versus yellow. As CYP3A enzymes are known carotenoid ketolases in other organisms, our results point to CYP3A80 as a strong candidate for a carotenoid ketolase in amphibians. Furthermore, in red frogs, the transcript encoding the carotenoid cleavage enzyme BCO2 is expressed at a low level or as a splice variant lacking key catalytic amino acids. This suggests that BCO2 function may be disrupted in red frogs, providing a mechanism whereby the accumulation of ketocarotenoids and their dietary precursors may be enhanced.

KEYWORDS
carotenoids, colour polymorphism, Dendrobatidae, ketolase

1 | INTRODUCTION

Carotenoids are common integumentary pigments in many animals, often responsible for yellow, orange, and red hues. A diverse class of over 600 pigments, carotenoids are acquired from the diet in animals and selectively absorbed, transported, and metabolized. As such, only a relatively small number (e.g., approximately 30 in birds; LaFountain et al., 2010; McGraw, 2006) have been found in coloured parts of the integument. Several of these are metabolic derivatives (converted carotenoids) of common dietary carotenoids, suggesting that many animals have the capacity to modify dietary carotenoids (Goodwin, 1986; McGraw, 2006). As the colours of carotenoids are due to their extended double bond system, metabolic transformations that alter the colour of a carotenoid typically do so by altering the number of conjugated double bonds in the molecule (McGraw, 2006).

The conversion of yellow dietary carotenoids to red ketocarotenoids represents one of the most common and dramatic mechanisms of colour modification in the animal kingdom. The addition of a ketone to a carotenoid at the C4 position of a β-ionone ring increases

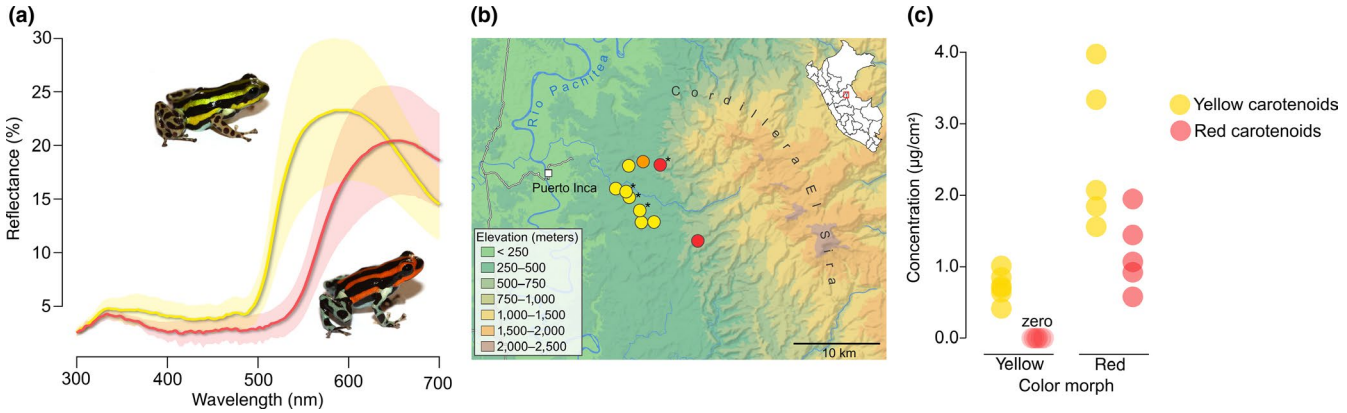

FIGURE 1 Overview of study system. (a) Dorsal reflectance spectra of yellow (n = 11) and red frogs (n = 9). Solid lines indicate mean, shaded areas indicate standard deviation. (b) Map of sampling area in central Peru. Dot colour indicates approximate frog colour at that site. Asterisks denote sampling localities for RNAseq samples. (c) Concentrations of red and yellow carotenoids in yellow (n = 6) and red (n = 5) *R. sirensis* morphs

the number of conjugated double bonds in the molecule, which shifts the light absorbance spectrum towards longer wavelengths and causes the carotenoid to become more red. Ketocarotenoid synthesis is known from a wide variety of organisms (Andrewes, Phaff, & Starr, 1976; Boussiba & Vonshak, 1991; Brockmann & Völker, 1934; Brush, 1990; Cunningham & Gantt, 2005; Twyman, Valenzuela, Literman, Andersson, & Mundy, 2016; Weaver, Cobine, & Hill, 2018; Wybouw et al., 2019) and in birds represents a major axis of variation in plumage colour (Friedman, McGraw, & Omland, 2014; McGraw, 2006). In addition, this type of modification may link carotenoid ornamentation to cellular function, as ketocarotenoid expression appears to be tightly coupled to mitochondria (Cantarero & Alonso-Alvarez, 2017) and perhaps mitochondrial respiration itself (Hill et al., 2019; Johnson & Hill, 2013).

Another aspect of carotenoid coloration involves accumulating sufficient carotenoid concentrations to impart bright colours. One way carotenoid accumulation can be enhanced is through the deactivation (either through low expression, sequence variation, or alternate splicing) of enzymes that are responsible for carotenoid breakdown, such as the β-carotene oxygenase enzymes BCMO1 and BCO2 (Lehnert et al., 2019; Li et al., 2014; von Lintig, 2010). Although this is typically thought of in relation to accumulating dietary carotenoids (Andrade et al., 2019; Eriksson et al., 2008; Lehnert et al., 2019), endogenously converted ketocarotenoids are also be susceptible to cleavage (Gazda et al., 2020). Thus, ketocarotenoid coloration may be linked not only to carotenoid ketolation, but also to the disruption of the pathways that lead to carotenoid breakdown, thereby facilitating accumulation.

In amphibians, ketocarotenoids are known from several species (Bonansea, Heit, & Vaira, 2017; Crothers et al., 2016; Czeczuga, 1980; Hee, Chun, & Young, 1975; Matsui, Marunouchi, & Nakamura, 2002), but the mechanisms leading to their production and/or accumulation have never been studied. In the species that do have ketocarotenoids, it is unclear whether ketolation occurs endogenously or if ketocarotenoids are taken directly from the diet. CYP2J19, the carotenoid ketolase in birds and turtles (Lopes et al., 2016; Mundy et al., 2016; Twyman et al., 2016), arose from a gene duplication that occurred in amniotes (Twyman et al., 2016). Consequently, CYP2J19 is not known from any amphibian, suggesting that carotenoid ketolation in amphibians would be through a distinct and presumably novel pathway.

Dendrobatid poison frogs are one of the most colour-diverse groups of vertebrates and are ideal for studying colour evolution in a nonavian system. Aside from advertising toxicity (Maan & Cummings, 2012; Saporito, Donnelly, Spande, & Garraffo, 2012), bright colours in this family also play key roles in mate choice (Dreher, Rodríguez, Cummings, & Pröhl, 2017; Summers, Symula, Clough, & Cronin, 1999), aggression (Crothers et al., 2016), mimicry (Symula, Schulte, & Summers, 2001), and population divergence and speciation (Twomey, Vestergaard, & Summers, 2014; Wang & Summers, 2010), yet the genetic mechanisms underlying coloration have only begun to be understood (Stuckert et al., 2019). Here, we study the pigmentary and genetic mechanisms underlying colour variation in the Sira poison frog *Ranitomeya sirensis* (Aichinger, 1991) (Figure 1a). *Ranitomeya sirensis* is a dendrobatid species widespread throughout the Amazonian lowlands and Andean foothills of central and southern Peru. Throughout most of its range, this species shows only modest colour variation ranging from yellow to lime green (Brown et al., 2011). However, near the Cordillera El Sira in central Peru, the species displays a red morph that was previously considered to be a distinct species (Aichinger, 1991; Brown et al., 2011). Here, we investigate this red/yellow polymorphism and demonstrate that it is due to the presence/absence of ketocarotenoids. This red colour persists in captivity without ketocarotenoid supplementation (Verleun, 2018), strongly indicating that ketocarotenoid synthesis is endogenous. We then investigate the genetic basis of this polymorphism using whole-transcriptome sequencing (RNAseq) to examine gene expression and sequence variation associated with ketocarotenoid coloration among red and yellow colour morphs.

2 | MATERIALS AND METHODS

2.1 | Sampling and colour measurements

Frogs were sampled between the town of Puerto Inca and the Cordillera El Sira in Huanuco, Peru. Sampling proceeded primarily along Quebrada Pintoyacu, a small stream flowing out of the Sira and into the lowlands near Puerto Inca. All sampling was done outside the Sira communal reserve. Details on reflectance spectrometry are given in the Supporting information.

2.2 | Pigment analysis

We analyzed skin and liver carotenoids and skin pteridines using thin-layer chromatography, methods identical to Twomey, Kain, et al. (2020). After reflectance measurements, frogs were euthanized with a lidocaine injection and skinned. All further procedures were done in darkness under the red light of a Petzl Tikka XP headlamp. To preserve skins for TLC, skins were dried onto mirror glass for approximately 2 hr (Juszczyk, 1952), removed with a blade and placed in a small paper envelope, and sealed in a 50 ml centrifuge tube along with silica gel desiccant and oxygen-absorbing packs. The tube was then flushed with an argon/nitrogen gas mixture, sealed, wrapped in aluminum foil to exclude light, and stored at −20°C until use.

Carotenoids were extracted from dried skins and livers by cutting the tissue into small pieces and soaking it for 2 hr in 200 µl 1:1 hexane:MTBE stabilized with 0.1% BHT. This extract was removed, and the tissue was soaked with an additional 50 µl extraction solvent for 15 min to ensure complete extraction. The two extracts were combined, dried to a volume of approximately 20 µl, and spotted onto 10 cm × 10 cm × 0.1 mm silica TLC plates. Additional details on TLC are given in the Supporting information. TLC plates were photographed after each development step for calculation of Rf values in each mobile phase, and after the final development, pigment spots were scraped and eluted with ethanol (30–200 µl depending on the intensity of the spot). We recorded absorbance spectra of eluted spots over 300–900 nm using a 10 µl minimum capacity quartz cuvette and a Stellarnet Silver-Nova spectrometer (190–1,100 nm range) and SPECTRAWIZ software version 5.33. Further tests were done to confirm carotenoid identity, such as saponification, borohydride reduction, and TLC with standards (Hudon, 1991; Rodriguez-Amaya, 2001). Further details on carotenoid identifications are given in the Supporting information. Carotenoid concentrations were calculated using the Beer-Lambert law, using published extinction coefficients when available (Britton, 1985). As it is not feasible to surgically separate coloured skin from black skin given the small size and intricate patterns of these frogs, we instead calculated the area of coloured skin in cm^2 from in-life dorsal photos of the frog. Therefore, concentration units are reported as amount per skin area rather than skin weight. Given that the pigment standards used were from natural sources, it was not possible to calculate a standard curve for calibrating carotenoid concentrations. Reported concentrations of carotenoids are not to be interpreted as absolute concentrations, but rather relative concentrations intended for comparisons among individuals within this study. Further details on pigment analyses and identifications are given in the Supporting information.

Pteridines were extracted by soaking the carotenoid-stripped skin pieces in 200 µl of an extraction solvent consisting of 70% ethanol with 3% ammonium hydroxide for 2 hr. The skin pieces were then removed, and 600 µl of chloroform was added to the extract and mixed. The sample was then centrifuged for 10 min at 16,200 *g*, which resulted in the formation of an upper, highly fluorescent layer containing pteridines (Frost & Robinson, 1984). This upper layer was drawn off and evaporated to dryness in a Speedvac. For TLC, the dried pteridine extract was resuspended in 40 µl of extraction solvent, and half of this was spotted onto a TLC plate (loading the entire extract overloaded the plate, resulting in poor separation). For pteridine TLC, we used combination silica-cellulose TLC plates (0.25 mm thick, cut to 10 × 10 cm), which, consistent with earlier studies, provided superior separation to silica or cellulose plates (Frost & Bagnara, 1978). Ascending TLC was done in two dimensions, the first using 14 ml propanol/7 ml 7% ammonium hydroxide as a mobile phase, the second using 10 ml butanol/3.5 ml water/1.5 ml glacial acetic acid as a mobile phase. When possible, absorbance spectra were taken in 0.1 M NaOH or 0.1 M HCl, as some pteridines undergo a spectral change in these two solvents which can be useful for identification (Frost, 1979). After each development, plates were photographed under black light (λmax 366 nm), which causes pteridines to fluoresce. For pigment standards, we used heads from wild type *Drosophila melanogaster* (drosopterin, a red pigment), and heads from the sepia mutant of *D. melanogaster* (sepiapterin and xanthopterin, both yellow pigments). TLC and spectral characteristics of pteridines isolated from *R. sirensis* and *Drosophila* are given in Table S1.

2.3 | RNA sequencing

We sampled livers and skins from six frogs (three yellow and three red) for RNA-sequencing (RNAseq). Red frogs were collected from a site at 378 m elevation, and yellow frogs were collected from a cluster of sites 5 km to the southwest at elevations ranging from 371–412 m. Frogs were captured in the field, transported to a local work area, and processed all on the same day over a 2 hr time period in the early afternoon. Working on ice, whole livers and skins were removed immediately after euthanasia and stored in RNAlater until extraction. For liver and skin samples, RNA was extracted using TRI reagent (Sigma-Aldrich) and the RNAeasy mini kit (Qiagen). For each liver sample, RNA sequencing libraries were made independently with the Illumina TruSeq RNA Library Preparation Kit, and paired-end, 76 bp reads were sequenced on an Illumina NextSeq 500 instrument at DNAVision. For skin samples, RNA sequencing libraries were made with the NEBNext Ultra RNA Library Prep kit, and paired end 150 bp reads were sequenced on an Illumina HiSeq 4000 instrument at Genewiz.

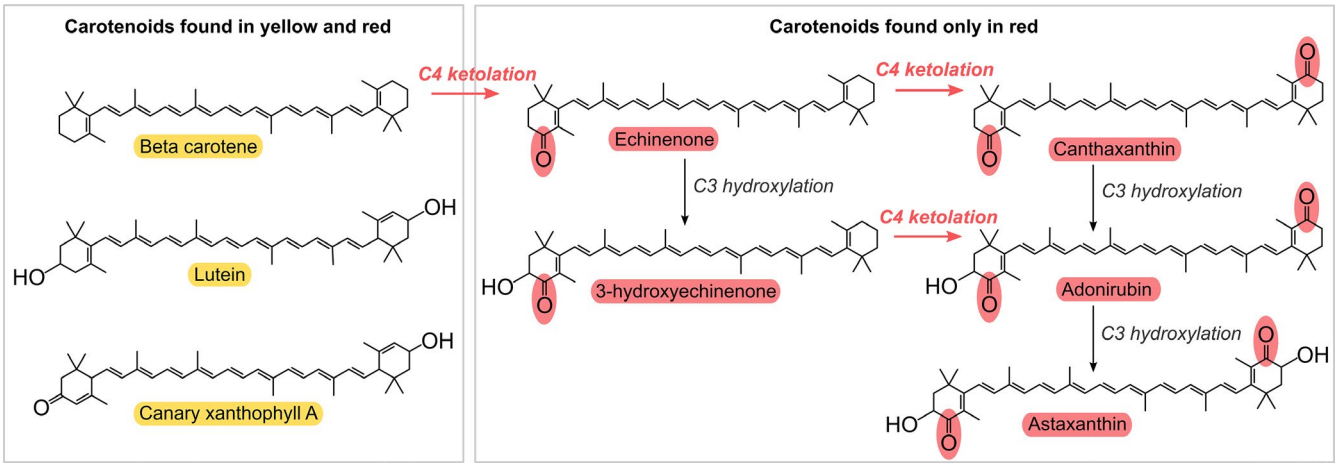

FIGURE 2 Carotenoids in red and yellow *Ranitomeya sirensis*. Carotenoid names are highlighted by their approximate colour. The three carotenoids on the left (β-carotene, lutein, and canary xanthophyll A) were found in all frogs regardless of colour. The five ketocarotenoids on the right were found only in red individuals. Putative conversion pathways from β-carotene to astaxanthin indicated by arrows, following proposed conversion pathway of CrtS (Ojima et al., 2006) [Colour figure can be viewed at wileyonlinelibrary.com]

2.4 | Sequence analysis

For transcriptome assembly, our general approach was to use multiple assemblers at a range of kmer values, using the EvidentialGene (Evigene) tr2aacds pipeline to merge multiple assemblies into a single nonredundant assembly for each tissue type. Assemblies were done separately by tissue (liver and skin) and by colour morph (red and yellow) to avoid the creation of colourwise chimeric transcripts. Our assembly protocol closely followed (Mamrot et al., 2017) except that we also used the SPAdes and Shannon assemblers in addition to Velvet/Oases, SOAPdenovo-Trans, and Trinity. Reads were aligned to the final assemblies with HISAT2 (version 2.1.0) (Kim, Langmead, & Salzberg, 2015) and differential expression (DE) analyses were done with the R package DESEQ2 using the Benjamin-Hochberg correction for multiple hypothesis testing (Love, Anders, & Huber, 2014).

We conducted a phylogenetic analysis (Figure 4) to resolve the position of *CrtS* and *CYP384A1* relative to the CYP3A family. For this analysis, we selected anuran P450 sequences from families 3, 4, 5, and 46 from the full cytochrome P450 data set (see Supporting information), and added additional Genbank sequences from the mouse, rat, human, chicken (*Gallus gallus*), painted turtle (*Chrysemys picta*), two poison frogs (*Oophaga pumilio* and *Ranitomeya imitator*), *CrtS* from red yeast, and *CYP384A1* from the spider mite *Tetranychus kanzawai*. Protein sequences were aligned with MAFFT (version 7.271) (Katoh & Standley, 2013) using the E-INS-I strategy and the "leave gappy regions" flag with the Blosum62 scoring matrix. Phylogenetic analyses were done in IQ-TREE (version 1.6.10) (Nguyen, Schmidt, von Haeseler, & Minh, 2014) with alrt = 1,000, ninit = 1,000, ntop = 1,000, nstop = 500, bb = 1,000, and the -allnni flag on. Resulting phylogenetic trees were midpoint rooted and viewed in FIGTREE (version 1.4.2) (Rambaut, 2014).

We also evaluated a set of 17 genes known from the literature to be involved in carotenoid coloration (Table S2). For each of these, we first evaluated whether the gene was present/absent in *R. sirensis*, and then manually inspected expression and read alignments for each individual and tissue to evaluate differential expression, nonsynonymous SNPs, and possible splice variants associated with red and yellow colour morphs.

3 | RESULTS AND DISCUSSION

3.1 | Geography of red/yellow polymorphism

Based on current sampling of the region and on previously published data (Brown et al., 2011), the yellow morph of *R. sirensis* is widespread throughout most of the Rio Pachitea drainage, including the lowlands between Puerto Inca and the Cordillera El Sira mountains (Figure 1b), with an approximate elevation range of 250–412 m. Near the foot of the Sira, the yellow morph shows a narrow, continuous transition to a red morph (Figure 1b), with a transition zone composed of orange individuals, which occurs over approximately 2 km of contiguous lowland habitat. This transition occurs before the elevation gradient; yellow populations were found up to 412 m elevation and red as low as 378 m. We emphasize that the red and yellow morphs do not overlap, only that there is overlap in the elevation records of the collection sites (e.g., some yellow individuals were collected along a low ridge with a slightly higher elevation than the red collection site). Although the red morph has been found as high as 1,560 m elevation in the Sira (Aichinger, 1991), we note that in other regions of Peru, yellow morphs are known to occur in highland habitats (e.g., up to 1,250 m elevation near Tingo Maria, Peru). Therefore, across the species as a whole, colour variation shows no relation to elevation.

3.2 | Red frogs are characterized by a suite of ketocarotenoids and high concentrations of yellow carotenoids

To identify the pigments that are responsible for the colour differences between red and yellow morphs, we isolated and characterized

skin carotenoids and pteridines. We found that pteridine extracts from red (n = 3) and yellow (n = 4) frogs were colourless, indicating that pteridines do not contribute to the red/yellow polymorphism (Figure S1). We further confirmed this result with thin-layer chromatography and found that the pteridine profiles of one red and three yellow frogs were identical and contained only colourless pteridines such as isoxanthopterin and pterin (Table S1). Notably, drosopterin, which contributes to orange/red colour in many organisms (Grether, Hudon, & Endler, 2001; McLean, Lutz, Rankin, Stuart-Fox, & Moussalli, 2017; Obika & Bagnara, 1964), was not found in any sample.

In contrast, red and yellow *R. sirensis* exhibited markedly different carotenoid profiles. In the dorsal skin and coloured patches of ventral skin, yellow *R. sirensis* (n = 6) had β-carotene, lutein, and canary xanthophyll A (Figure 2, Figure S2), all of which are yellow carotenoids, with absorbance peaks at 440–450 nm. Red frogs (n = 5) also had these three yellow carotenoids, but at much higher concentrations (Figure 1c, Figure S2). In addition, all red frogs had the following C4 ketocarotenoids: echinenone, 3-hydroxyechinenone, canthaxanthin, adonirubin, and astaxanthin (Figure 2, Figure S2). All red frogs also contained an unidentified ketocarotenoid with spectral similarity to alpha-doradexanthin (reverting to a lutein-like absorbance spectrum upon borohydride reduction), and two red frogs contained low amounts of a red carotenoid with similarity to eschscholtzxanthin (no change in spectrum upon borohydride reduction). See Supporting information for details on carotenoid identifications.

The carotenoid profiles of orange frogs were intermediates: five orange frogs had the entire suite of ketocarotenoids exhibited by red frogs, but in lower concentrations, and one orange frog (Figure S2) had high concentrations of yellow carotenoids but lacked ketocarotenoids. Overall, red coloration in *R. sirensis* is highly correlated with the presence of multiple ketocarotenoids and high concentrations of yellow carotenoids.

3.3 | *CYP3A80* is an ideal candidate for a carotenoid ketolase

Neither β-cryptoxanthin nor zeaxanthin, which are potential precursors of several of the observed C4 ketocarotenoids, were detected in the skins of any frog. The most plausible source of ketocarotenoids in red frogs is thus C4 ketolation/C3 hydroxylation of β-carotene (Figure 2), although lutein cannot be ruled out as a precursor given that some birds may convert lutein to zeaxanthin (McGraw, 2006). It has been hypothesized that ketocarotenoids are formed in the liver (Ge et al., 2015; del Val et al., 2009) and in most birds studied to date, expression of CYP2J19 is low or undetectable in the integument but differentially expressed in livers (Twyman, Prager, Mundy, & Andersson, 2018, but see Lopes et al., 2016). We therefore examined carotenoid contents of the livers of two red frogs with abundant skin ketocarotenoids, and found that ketocarotenoids were present (Figure S3). Although this suggests that carotenoid ketolation occurs in the liver rather than the skin, an alternative possibility is that ketocarotenoids are formed locally in the skin and recirculated throughout the body, including the liver (e.g., for breakdown). Therefore, to account for the possibility that ketolation could occur in the skin, gene expression analyses were done on both liver and skin tissues.

To investigate the genetic basis of ketocarotenoid coloration, we studied differential gene expression in the livers and skins of three red and three yellow *R. sirensis* using RNAseq. From liver tissues, we sequenced ~350 million paired-end 75 bp reads (mean = 59.4 million reads/sample); for skin tissues, we sequenced a total of ~335 million paired-end 150 bp reads (mean = 56 million reads/sample) (Table S3). We used a multiassembler approach to transcriptome assembly where multiple assemblies were made for each tissue type and merged using the EvidentialGene pipeline (see Materials and Methods). We produced two final assemblies (one per tissue type) for downstream analyses (assembly metrics shown in Table S4).

In skins, we found 168 transcripts with significant differential expression between red and yellow morphs (68 higher in red, 100 higher in yellow; adjusted p < .05, Figure 3b, Table S5). Of these, only one transcript (*CYP2G1-like*, p = .043, Table S5) had the expression pattern (red > yellow) and potential oxygenase activity expected of a carotenoid ketolase. When we investigated this transcript, we found that the translation gave only a fragmentary sequence (69 amino acids) fully contained within a complete transcript (436 amino acids) corresponding to *CYP2QT.8C*, which was not differentially expressed in our P450-specific expression analysis of skin tissue (p = .852, Table S6), indicating that the initial result is probably a read-mapping artefact.

In livers, we found 164 transcripts with significant differential expression between red and yellow morphs (109 higher in red, 55 higher in yellow; adjusted p < .05, Figure 3b, Table S5). Of these, two transcripts had the expression pattern (red > yellow) and potential oxygenase activity expected of a carotenoid ketolase, both belonging to the cytochrome P450 class of enzymes (*CYP3A80*, Figure 3a and *CYP46A.4*). The *CYP46A.4* transcript had a marginal p-value (p = .032), attributed to the relatively high intramorph variation in expression levels. This transcript encodes the enzyme cholesterol 24-hydroxylase, which is involved in bile acid synthesis via hydroxylation of cholesterol side chains (Mast et al., 2008). Overall, our expression data and modelling both suggest that CYP46A.4 is an unlikely candidate for a carotenoid ketolase.

By contrast, CYP3A80 is an ideal candidate for a carotenoid ketolase. In addition to the relatively strong morph-based, tissue-specific differential expression of its transcript (livers; Log2FC = 1.6, p = .007; Figure 3a), enzymes of the CYP3A class are known carotenoid ketolases in other organisms, including red yeast (CrtS, Ojima et al., 2006 and spider mites (CYP384A1, Wybouw et al., 2019) (Figure 4). In both examples, β-carotene is converted into a suite of ketocarotenoids identical to those of *R. sirensis* (Ojima et al., 2006; Veerman, 1970; Figure 2) and thus the conversion pathways appear to be remarkably similar if not identical in all three cases. More generally, CYP3A enzymes have exceptional flexibility and broad substrate specificity (Rendic & Guengerich, 2015). β-carotene, which has two

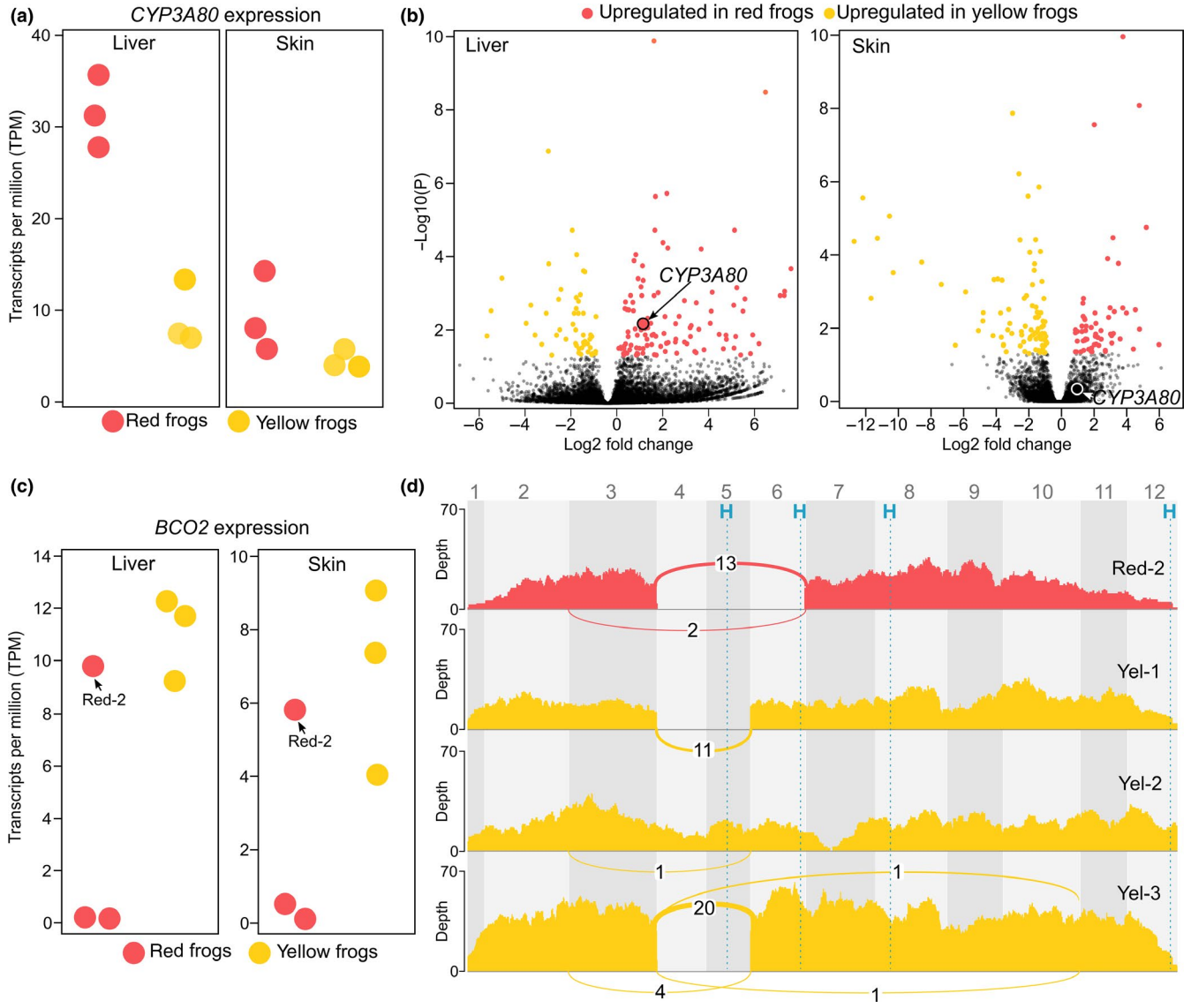

FIGURE 3 Differential expression of *CYP3A80* and *BCO2* splice variant. (a) Expression of the candidate ketolase *CYP3A80* in livers and skins of red (n = 3) and yellow (n = 3) *Ranitomeya sirensis*. (b) Volcano plots of effect size (log2 fold change, x axis) and statistical significance (-log10 p-value, y axis) for transcripts in the differential expression analyses. Each transcript is represented by a dot; transcripts significantly upregulated in red frogs shown in red and those upregulated in yellow frogs shown in yellow. (c) Expression of *β-carotene oxygenase 2* (*BCO2*) in livers and skins of red and yellow frogs. (d) Sashimi plot showing *BCO2* alternate splice variants found in liver tissue (sashimi plot for skin shown in Figure S5). Coloured regions indicate per-base read counts (y axis); coloured arcs and numbers indicate junction-spanning reads and their counts. Vertical grey regions indicate exon boundaries; vertical blue dashed lines indicate position of conserved histidine residues

β-ionone rings, appears to be an ideal substrate, as CYP3A enzymes in mammals are able to perform C4-ketolations on the β-ionone rings of retinoic acid and fenretinide (Figure 4, Figure S4) (Cooper et al., 2011; Marill, Capron, Idres, & Chabot, 2002; Marill, Cresteil, Lanotte, & Chabot, 2000; Martini & Murray, 1993). Modelling of *R. sirensis* CYP3A80 reveals a substrate cavity well-suited to a large and hydrophobic molecule such as β-carotene. Overall, there is ample evidence to suggest that CYP3A enzymes are broadly capable of carotenoid ketolation (Figure 4).

Of the six known carotenoid ketolase enzymes, three (CrtW, known from marine bacteria; CrtO, known from the alga *Haematococcus pluvialis*; and CYP2J19, known from birds and turtles) appear to function solely as ketolases, converting β-carotene to canthaxanthin either directly or through echinenone as an intermediate (Henke, Heider, Peters-Wendisch, & Wendisch, 2016; Lopes et al., 2016). In these taxa, the 3-hydroxy, 4-keto carotenoids (e.g., adonirubin, astaxanthin, 3-hydroxyechinenone) are produced either through a secondary hydroxylase enzyme (e.g., CrtZ), or by ketolation of 3-hydroxy precursors such as β-cryptoxanthin and zeaxanthin (del Val et al., 2009). By contrast, in the flowering plant *Adonis aestivalis*, ketocarotenoids are formed by the combined action of a hydroxylase (CBFD) and dehydrogenase (HBFD) (Cunningham & Gantt, 2011), making this pathway unique in ketocarotenoid biosynthesis. Finally, CrtS (a.k.a. "astaxanthin synthase",

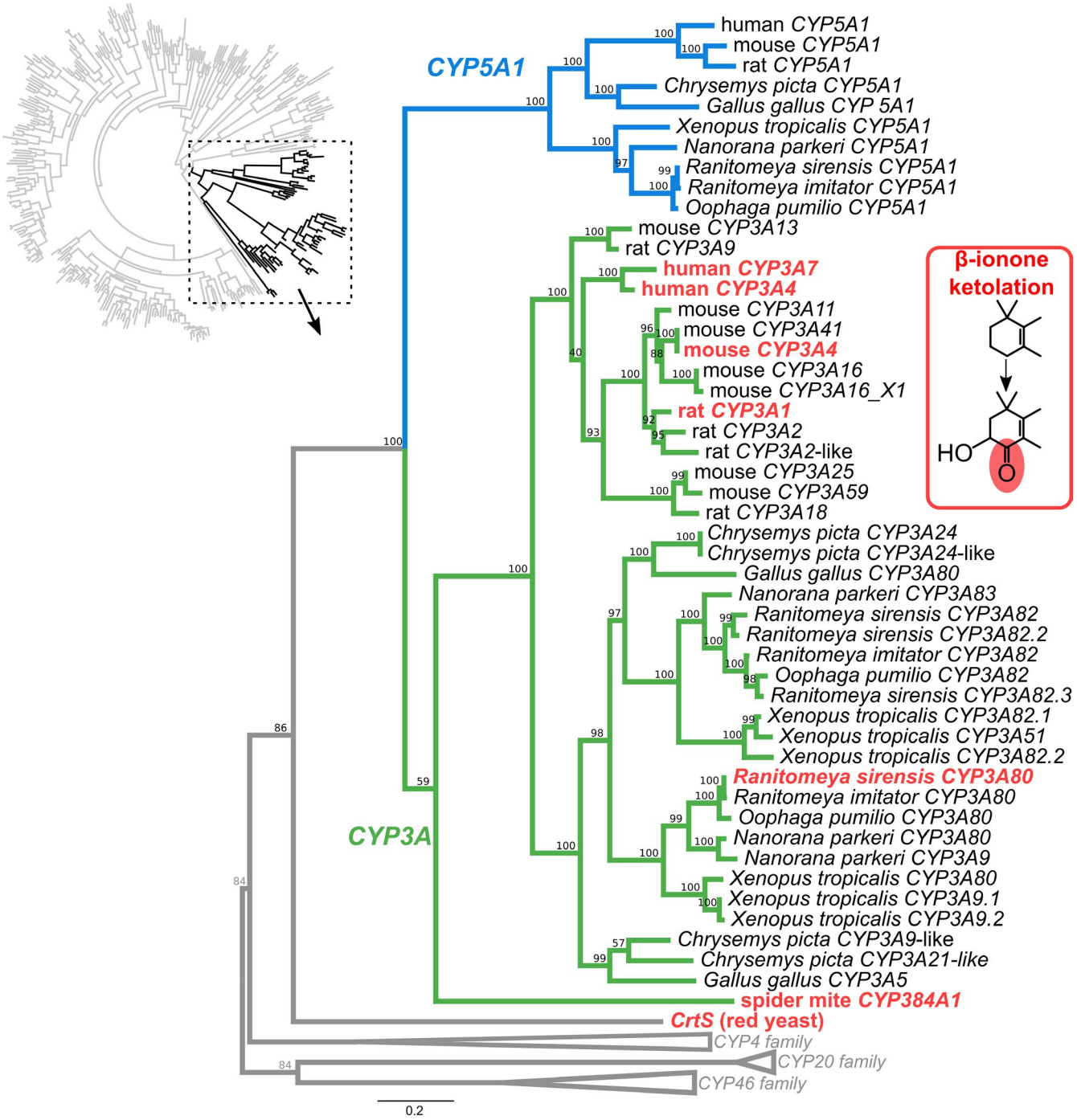

FIGURE 4 Amino acid phylogeny of *CYP3A80*, the candidate carotenoid ketolase in *Ranitomeya sirensis*. Top left shows the phylogeny of anuran cytochrome P450s (detailed phylogeny with terminal names given in Figure S7). The part highlighted in bold, which contains CYP3A and related families, is expanded on right. Terminals marked in red are those where ketolation of β-ionone rings has been shown or is suspected. Note that the *CYP3A80* sequence is identical between red and yellow *R. sirensis* morphs, therefore only a single terminal is shown. The numbers over branches are bootstrap values based on 1,000 ultrafast bootstrap replicates in IQ-TREE [Colour figure can be viewed at wileyonlinelibrary.com]

or Asy) from red yeast and CYP384A1 from spider mites (Wybouw et al., 2019) are both members of the CYP3A class and appear to function as carotenoid C4-ketolase/C3-hydroxylase enzymes. In CrtS, the mode of conversion involves a double hydroxylation at carbon 4, followed by a single hydroxylation at carbon 3, which results a suite of 3-hydroxy, 4-keto carotenoids and can also produce 4-keto carotenoids lacking hydroxyl groups (e.g., echinenone and canthaxanthin) under certain conditions (Ojima et al., 2006). Given that the ketocarotenoid profiles are identical among red yeast, spider mites, and *Ranitomeya sirensis*, this strongly suggests that dual ketolation/hydroxylation function is characteristic of CYP3A carotenoid ketolases.

3.4 | BCO2 expression and splice variants

In a number of animal species, β-carotene oxygenase 2 (BCO2) is a major regulator of carotenoid coloration (Amengual et al., 2011; Andrade et al., 2019; Gazda et al., 2020; Lehnert et al., 2019; Palczewski, Amengual, Hoppel, & von Lintig, 2014). This enzyme results in the asymmetrical cleavage of β-carotene, lutein, and zeaxanthin to form apocarotenoids (von Lintig, 2010). Because this cleavage results in the formation of predominantly colourless molecules, BCO2 can regulate carotenoid coloration by reducing carotenoid levels when it is highly expressed, and facilitating carotenoid accumulation when it is weakly expressed or disrupted (Toews, Hofmeister, & Taylor, 2017).

One of the major pigmentary differences between red and yellow frogs is in the concentration of yellow carotenoids (e.g., lutein and β-carotene), which is nearly 3-fold higher on average in red frogs (Figure 1c). In our analysis of 17 candidate carotenoid genes identified from the literature, only one—*BCO2*—showed differences between red and yellow morphs (Table S2). Specifically, we found that in both skin and liver tissue, two of the three red frogs had negligible *BCO2* expression (Figure 3c), while the third expressed an alternate splice that skips exons 4–6 (Figure 3d). In contrast, yellow frogs predominantly expressed a full-length transcript or an alternate splice skipping exons 4 and 5 (Figure 3d). The latter splice variant, corresponding to "isoform D" in humans (dela Seña et al., 2016), lacks one of the four conserved histidine residues that coordinate binding of the catalytic iron, but has been shown to be functional in humans (Kim, Yeom, & Oh, 2011). It is unknown whether the red splice variant (lacking exons 4–6) would be functional, but given that it lacks two of the four conserved histidines we expect that its function should at least be impaired. Therefore, the accumulation of yellow carotenoids in red frogs may be due to the low expression of *BCO2* and/or the expression of a non- or partly functional splice variant.

Recent work further suggests that the accumulation of red ketocarotenoids may also be regulated by *BCO2*. Lehnert et al. (2019) found that in Chinook salmon, which gain red muscle colour through the accumulation of dietary ketocarotenoids, colour variation is strongly associated with both expression and sequence variation in *BCO2*. Specifically, the white morph of Chinook salmon, which lacks ketocarotenoids, has high *BCO2* expression in muscle tissue, whereas the typical red Chinook salmon have low *BCO2* expression. Additionally, Gazda et al. (2020) found that a loss-of-function mutation in *BCO2* was associated with the accumulation of endogenously converted ketocarotenoids in bare parts of red urucum canaries. Together, this suggests that disruption or downregulation of *BCO2* is a prerequisite for ketocarotenoid accumulation, and that *BCO2* is capable of breaking down ketocarotenoids when it is highly expressed and/or functional.

Together, these results suggest that *BCO2* could have two major impacts on the production and accumulation of ketocarotenoids. First, *BCO2* disruption/downregulation at the site of ketocarotenoid synthesis (e.g., liver) would lead to an accumulation of yellow dietary carotenoids that serve as ketocarotenoid precursors, which, when combined with increase expression of the ketolase, would result in increased ketocarotenoid synthesis. Second, *BCO2* disruption/downregulation at the site of carotenoid accumulation (e.g., skin) would facilitate the accumulation of both dietary and converted carotenoids. We hypothesize that in *R. sirensis* this disruption is regulated by alternate splicing and/or low expression of *BCO2* both in the livers (Figure 3) and skin (Figure 3, Figure S5). In our hypothesized scenario, ketocarotenoid coloration would reflect an interplay between carotenoid accumulation regulated by *BCO2* and carotenoid ketolation regulated by *CYP3A80* (Figure S6). Such an interaction could explain how such drastic pigmentary differences are seen in red and yellow *R. sirensis* despite modest expression differences in the putative ketolase.

3.5 | Ecological implications

Colour polymorphisms—two or more distinct, genetically determined colour morphs within a single interbreeding population (McKinnon & Pierotti, 2010)—can have important biological consequences. When coupled with variation in mating preferences, they can lead to assortative mating, reproductive isolation, and speciation (Gray & McKinnon, 2007; McLean & Stuart-Fox, 2014). Aposematic species also frequently have colour polymorphisms, often due to locally strong but geographically variable positive frequency dependent selection (Chouteau & Angers, 2011; Mallet & Barton, 1989). Such a selection regime typically results in two parapatric morphs occupying distinct geographic areas but joined by a narrow cline composed of intermediate individuals (Barton & Hewitt, 1985).

The red and yellow morphs of *R. sirensis* transition over a narrow zone of approximately 2 km in what appears to be a classic cline. Phenotypic clines of similar widths have been found in other species of poison frogs (Twomey, Vestergaard, Venegas, & Summers, 2015; Yang, Blomenkamp, Dugas, Richards-Zawacki, & Pröhl, 2019) and available evidence points to these clines being maintained by strong natural selection (Chouteau & Angers, 2012) and mate choice (Twomey et al., 2014, but see Yang et al., 2019). Given that ketocarotenoids are known to be particularly attractive sexual signals in birds (Weaver, Santos, Tucker, Wilson, & Hill, 2018), future research should determine whether there is colour-based assortative mating in *R. sirensis* and whether this contributes to the maintenance of such a narrow phenotypic cline.

Our results suggest that there could be at least three genetic mechanisms underlying the colour cline in *R. sirensis:* (a) regulatory variation in CYP3A80 and (b) regulatory variation in BCO2, regulating expression of these genes; and (c) splice-site mutations regulating splice variation in BCO2. Orange frogs may therefore represent a mixture of red and yellow alleles within the transition zone. This system would therefore represent an ideal opportunity for exploring how population genetic structure and allelic variation could link to variation in an ecologically relevant warning signal.

Despite differences in the proposed genetic mechanisms of ketocarotenoids in birds and poison frogs, the signalling functions

may be similar. In another poison frog species, *Oophaga pumilio*, whose carotenoid profile bears striking similarity to red *R. sirensis* (Crothers et al., 2016), mate choice is regulated in large part by colour (Dreher et al., 2017; Maan & Cummings, 2008, 2009; Richards-Zawacki, Wang, & Summers, 2012; Summers et al., 1999). This raises the possibility that ketocarotenoids, as in birds, represent sexual signals in poison frogs. However, given that bright coloration in poison frogs also serves as a warning signal to predators (Darst & Cummings, 2006; Maan & Cummings, 2012; Santos, Coloma, & Cannatella, 2003; Summers & Clough, 2001), ketocarotenoid synthesis may simply be a response to natural selection for being red. Future investigations into the signalling functions of carotenoids in aposematic species must therefore consider their role in signalling individual quality to potential mates as well as advertising toxicity to potential predators.

In conclusion, by combining field sampling, pigment analysis, and transcriptome sequencing, our study has traced a natural colour polymorphism to the presence/absence of specific skin pigments and variation in gene expression that together implicate CYP3A80 as a novel carotenoid ketolase. Although birds remain the best-studied group of vertebrates in terms of carotenoid coloration, our study provides groundwork for studying ketocarotenoid coloration in amphibians, a group of ca. 8,000 species, many of which have bright coloration that serves diverse signalling functions. Comparative data on other amphibian species will allow for testing whether ketocarotenoid-based colours typically evolve through recurrent use of CYP3A80 as a carotenoid ketolase or through alternative mechanisms such as dietary sequestration or alternate pathways for endogenous conversion.

To date, there have been no direct experiments (e.g., molecular cloning) confirming the function of any proposed vertebrate carotenoid ketolase, and thus the functions of both CYP3A80 and CYP2J19 are still hypotheses based on strong circumstantial evidence. Such assays would also be valuable in determining the precise precursor-product relationships between dietary and converted carotenoids, which is important for determining whether a single enzyme can account for all observed ketocarotenoids or if secondary enzymes (e.g., hydroxylases) could be involved. Future studies on the subcellular location (e.g., mitochondria) of these enzymes will also help clarify how ketocarotenoid synthesis relates to overall cellular function and will strengthen our understanding of how carotenoid-based colours serve as honest signals.

ACKNOWLEDGEMENTS

We thank Joy Jordan Paredes Panduro for help in the field, Kevin McGraw for providing pigment standards, and Dag Treer, Margo Maex, Franky Bossuyt, Eduardo Eizirik, and Theo Verleun for discussion and feedback on the project. Collections and export were done under permit numbers 0266-2011-AG-DGFFS-DGEFFS, 0407-2012-AG-DGFFS-DGEFFS, 068-2016-SERFOR/DGSPFFS, 034-2017-SERFOR/DGGSPFFS, and 009-2013-MINAGRI-DGFFS/DGEFFS issued by the Peruvian government. This work was supported by CAPES, Brazil (Science Without Borders programme) to E.T. and by the Fonds voor Wetenschappelijk Onderzoek (FWO) Vlaanderen (grant G0D6618N) and Strategic Research Programme of the Vrije Universiteit Brussel (grant SRP30).

AUTHOR CONTRIBUTIONS

E.T., I.V.B., and S.C.F. designed the study. E.T. performed the research. E.T., and J.D.J. analysed data. E.T., J.D.J., I.V.B., and S.C.F. wrote the paper.

DATA AVAILABILITY STATEMENT

RNAseq reads have been deposited in the European Nucleotide archive, study accession PRJEB37981. Other data (transcriptome assemblies, annotations, sequence alignments, expression results, and reflectance spectra) has been deposited in the Dryad Digital Repository (https://doi.org/10.5061/dryad.wpzgmsbj2; Twomey, Johnson, Johnson, Castroviejo-Fisher, & Van Bocxlaer, 2020).

ORCID

Evan Twomey https://orcid.org/0000-0002-8001-4343

REFERENCES

Aichinger, M. (1991). A new species of poison-dart frog (Anura: Dendrobatidae) from the Serrania de Sira. *Peru. Herpetologica*, *47*(1), 1–5.

Amengual, J., Lobo, G. P., Golczak, M., Li, H. N. M., Klimova, T., Hoppel, C. L., … von Lintig, J. (2011). A mitochondrial enzyme degrades carotenoids and protects against oxidative stress. *The FASEB Journal*, *25*(3), 948–959. https://doi.org/10.1096/fj.10-173906

Andrade, P., Pinho, C., Pérez i de Lanuza, G., Afonso, S., Brejcha, J., Rubin, C.-J., … Carneiro, M. (2019). Regulatory changes in pterin and carotenoid genes underlie balanced color polymorphisms in the wall lizard. *Proceedings of the National Academy of Sciences*, *116*(12), 5633–5642. https://doi.org/10.1073/pnas.1820320116

Andrewes, A. G., Phaff, H. J., & Starr, M. P. (1976). Carotenoids of *Phaffia rhodozyma*, a red-pigmented fermenting yeast. *Phytochemistry*, *15*(6), 1003–1007. https://doi.org/10.1016/S0031-9422(00)84390-3

Barton, N. H., & Hewitt, G. (1985). Analysis of hybrid zones. *Annual Review of Ecology and Systematics*, *16*, 113–148. https://doi.org/10.1146/annurev.es.16.110185.000553

Bonansea, M. I., Heit, C., & Vaira, M. (2017). Pigment composition of the bright skin in the poison toad *Melanophryniscus rubriventris* (Anura: Bufonidae) from Argentina. *Salamandra*, *53*(1), 142–147.

Boussiba, S., & Vonshak, A. (1991). Astaxanthin accumulation in the green alga *Haematococcus pluvialis*. *Plant and Cell Physiology*, *32*(7), 1077–1082. https://doi.org/10.1093/oxfordjournals.pcp.a078171

Britton, G. (1985). General carotenoid methods. In J. H. Law & H. C. Rilling (Eds.), *Methods in enzymology* (vol. III, pp. 113–149). Cambridge, MA: Academic Press.

Brockmann, H., & Völker, O. (1934). Der gelbe Federfarbstoff des Kanarienvogels *[Serinus canaria canaria (L.)]* und das Vorkommen von Carotinoiden bei Vögeln. *Hoppe-Seyler´s Zeitschrift Für Physiologische Chemie*, *224*(5–6), 193–215. https://doi.org/10.1515/bchm2.1934.224.5-6.193

Brown, J. L., Twomey, E., Amézquita, A., De souza, M. B., Caldwell, J. P., Lötters, S., … Summers, K. (2011). A taxonomic revision of the Neotropical poison frog genus *Ranitomeya* (Amphibia: Dendrobatidae). *Zootaxa*, *3083*, 1–120. https://doi.org/10.11646/zootaxa.3083.1.1

Brush, A. H. (1990). Metabolism of carotenoid pigments in birds. *The FASEB Journal*, *4*(12), 2969–2977. https://doi.org/10.1096/fasebj.4.12.2394316

Cantarero, A., & Alonso-Alvarez, C. (2017). Mitochondria-targeted molecules determine the redness of the zebra finch bill. *Biology Letters*, *13*(10), 20170455. https://doi.org/10.1098/rsbl.2017.0455

Chouteau, M., & Angers, B. (2011). The role of predators in maintaining the geographic organization of aposematic signals. *The American Naturalist*, *178*(6), 810–817. https://doi.org/10.1086/662667

Chouteau, M., & Angers, B. (2012). Wright's shifting balance theory and the diversification of aposematic signals. *PLoS One*, *7*(3), e34028. https://doi.org/10.1371/journal.pone.0034028

Cooper, J. P., Hwang, K., Singh, H., Wang, D., Reynolds, C. P., Curley Jr, R. W., … Kang, M. H. (2011). Fenretinide metabolism in humans and mice: Utilizing pharmacological modulation of its metabolic pathway to increase systemic exposure. *British Journal of Pharmacology*, *163*(6), 1263–1275. https://doi.org/10.1111/j.1476-5381.2011.01310.x

Crothers, L., Saporito, R. A., Yeager, J., Lynch, K., Friesen, C., Richards-Zawacki, C. L., … Cummings, M. (2016). Warning signal properties covary with toxicity but not testosterone or aggregate carotenoids in a poison frog. *Evolutionary Ecology*, *30*, 601–621. https://doi.org/10.1007/s10682-016-9830-y

Cunningham, F. X., & Gantt, E. (2005). A study in scarlet: Enzymes of ketocarotenoid biosynthesis in the flowers of *Adonis aestivalis*: *Adonis* β-ring oxygenases. *The Plant Journal*, *41*(3), 478–492. https://doi.org/10.1111/j.1365-313X.2004.02309.x

Cunningham, F. X., & Gantt, E. (2011). Elucidation of the pathway to astaxanthin in the flowers of *Adonis aestivalis*. *The Plant Cell*, *23*(8), 3055–3069. https://doi.org/10.1105/tpc.111.086827

Czeczuga, B. (1980). Investigations on carotenoids in amphibia—II. Carotenoids occurring in various parts of the body of certain species. *Comparative Biochemistry and Physiology Part B: Comparative Biochemistry*, *65*(4), 623–630. https://doi.org/10.1016/0305-0491(80)90170-4

Darst, C. R., & Cummings, M. E. (2006). Predator learning favours mimicry of a less-toxic model in poison frogs. *Nature*, *440*(7081), 208–211.

del Val, E., Senar, J. C., Garrido-Fernández, J., Jarén, M., Borràs, A., Cabrera, J., & Negro, J. J. (2009). The liver but not the skin is the site for conversion of a red carotenoid in a passerine bird. *Naturwissenschaften*, *96*(7), 797–801. https://doi.org/10.1007/s00114-009-0534-9

dela Seña, C., Sun, J., Narayanasamy, S., Riedl, K. M., Yuan, Y., Curley, R. W., … Harrison, E. H. (2016). Substrate specificity of purified recombinant chicken β-Carotene 9′,10′-oxygenase (BCO2). *Journal of Biological Chemistry*, *291*(28), 14609–14619. https://doi.org/10.1074/jbc.M116.723684

Dreher, C. E., Rodríguez, A., Cummings, M. E., & Pröhl, H. (2017). Mating status correlates with dorsal brightness in some but not all poison frog populations. *Ecology and Evolution*, *7*(24), 10503–10512. https://doi.org/10.1002/ece3.3531

Eriksson, J., Larson, G., Gunnarsson, U., Bed'hom, B., Tixier-Boichard, M., Strömstedt, L., … Andersson, L. (2008). Identification of the *Yellow Skin* gene reveals a hybrid origin of the domestic chicken. *PLOS Genetics*, *4*(2), e1000010. https://doi.org/10.1371/journal.pgen.1000010

Friedman, N. R., McGraw, K. J., & Omland, K. E. (2014). Evolution of carotenoid pigmentation in caciques and meadowlarks (Icteridae): Repeated gains of red plumage coloration by carotenoid C4-oxygenation. *Evolution*, *68*(3), 791–801. https://doi.org/10.1111/evo.12304

Frost, S. K. V. (1979). *Developmental aspects of pigmentation in the Mexican leaf frog*, Pachymedusa dacnicolor. Tucson, AZ:University of Arizona.

Frost, S., & Bagnara, J. T. (1978). Separation of pteridines by thin-layer chromatography on combination plates. *Journal of Chromatography A*, *153*(1), 279–283. https://doi.org/10.1016/S0021-9673(00)89886-6

Frost, S. K., & Robinson, S. J. (1984). Pigment cell differentiation in the fire-bellied toad, *Bombina orientalis*. I. Structural, chemical, and physical aspects of the adult pigment pattern. *Journal of Morphology*, *179*(3), 229–242.

Gazda, M. A., Toomey, M. B., Araújo, P. M., Lopes, R. J., Afonso, S., Myers, C. A., … Carneiro, M. (2020). Genetic basis of de novo appearance of carotenoid ornamentation in bare parts of canaries. *Molecular Biology and Evolution*, *37*(5), 1317–1328. https://doi.org/10.1093/molbev/msaa006

Ge, Z., Johnson, J. D., Cobine, P. A., McGraw, K. J., Garcia, R., & Hill, G. E. (2015). High concentrations of ketocarotenoids in hepatic mitochondria of *Haemorhous mexicanus*. *Physiological and Biochemical Zoology*, *88*(4), 444–450. https://doi.org/10.1086/681992

Goodwin, T. W. (1986). Metabolism, nutrition, and function of carotenoids. *Annual Review of Nutrition*, *6*(1), 273–297. https://doi.org/10.1146/annurev.nu.06.070186.001421

Gray, S. M., & McKinnon, J. S. (2007). Linking color polymorphism maintenance and speciation. *Trends in Ecology & Evolution*, *22*(2), 71–79. https://doi.org/10.1016/j.tree.2006.10.005

Grether, G. F., Hudon, J., & Endler, J. A. (2001). Carotenoid scarcity, synthetic pteridine pigments and the evolution of sexual coloration in guppies (*Poecilia reticulata*). *Proceedings of the Royal Society B: Biological Sciences*, *268*(1473), 1245–1253. https://doi.org/10.1098/rspb.2001.1624

Hee, C. S., Chun, C. U., & Young, C. I. (1975). Studies on the carotenoid pigment in abdominal skin of *Bombina orientalis* (III). Occurrence of 3-hydroxy-canthaxanthin in the abdominal skin of *Bombina orientalis*. *Journal of the Korean Chemical Society*, *19*(1), 34–37.

Henke, N. A., Heider, S. A. E., Peters-Wendisch, P., & Wendisch, V. F. (2016). Production of the marine carotenoid astaxanthin by metabolically engineered *Corynebacterium glutamicum*. *Marine Drugs*, *14*(7), https://doi.org/10.3390/md14070124

Hill, G. E., Hood, W. R., Ge, Z., Grinter, R., Greening, C., Johnson, J. D., … Zhang, Y. (2019). Plumage redness signals mitochondrial function in the house finch. *Proceedings of the Royal Society B: Biological Sciences*, *286*(1911), 20191354. https://doi.org/10.1098/rspb.2019.1354

Hudon, J. (1991). Unusual carotenoid use by the Western Tanager (*Piranga ludoviciana*) and its evolutionary implications. *Canadian Journal of Zoology*, *69*(9), 2311–2320. https://doi.org/10.1139/z91-325

Johnson, J. D., & Hill, G. E. (2013). Is carotenoid ornamentation linked to the inner mitochondria membrane potential? A hypothesis for the maintenance of signal honesty. *Biochimie*, *95*(2), 436–444. https://doi.org/10.1016/j.biochi.2012.10.021

Juszczyk, W. (1952). The preservation of natural colors in skin preparations of certain Amphibia. *Copeia*, *1952*(1), 33–38. https://doi.org/10.2307/1437621

Katoh, K., & Standley, D. M. (2013). MAFFT multiple sequence alignment software version 7: Improvements in performance and usability. *Molecular Biology and Evolution*, *30*(4), 772–780. https://doi.org/10.1093/molbev/mst010

Kim, D., Langmead, B., & Salzberg, S. L. (2015). HISAT: A fast spliced aligner with low memory requirements. *Nature Methods*, *12*(4), 357. https://doi.org/10.1038/nmeth.3317

Kim, Y.-S., Yeom, S.-J., & Oh, D.-K. (2011). Production of β-apo-10′-carotenal from β-carotene by human β-carotene-9′,10′-oxygenase expressed in *E. coli*. *Biotechnology Letters*, *33*(6), 1195–1200. https://doi.org/10.1007/s10529-011-0556-1

LaFountain, A. M., Kaligotla, S., Cawley, S., Riedl, K. M., Schwartz, S. J., Frank, H. A., & Prum, R. O. (2010). Novel methoxy-carotenoids from the burgundy-colored plumage of the Pompadour Cotinga *Xipholena punicea*. *Archives of Biochemistry and Biophysics*, *504*(1), 142–153. https://doi.org/10.1016/j.abb.2010.08.006

Lehnert, S. J., Christensen, K. A., Vandersteen, W. E., Sakhrani, D., Pitcher, T. E., Heath, J. W., … Devlin, R. H. (2019). Carotenoid pigmentation in salmon: Variation in expression at *BCO2-l* locus controls a key fitness trait affecting red coloration. *Proceedings of the*

Royal Society B: Biological Sciences, *286*(1913), 20191588. https://doi.org/10.1098/rspb.2019.1588

Li, B., Vachali, P. P., Gorusupudi, A., Shen, Z., Sharifzadeh, H., Besch, B. M., … Bernstein, P. S. (2014). Inactivity of human β, β-carotene-9′,10′-dioxygenase (BCO2) underlies retinal accumulation of the human macular carotenoid pigment. *Proceedings of the National Academy of Sciences of the United States of America*, *111*(28), 10173–10178. https://doi.org/10.1073/pnas.1402526111

Lopes, R. J., Johnson, J. D., Toomey, M. B., Ferreira, M. S., Araujo, P. M., Melo-Ferreira, J., … Carneiro, M. (2016). Genetic basis for red coloration in birds. *Current Biology*, *26*(11), 1427–1434. https://doi.org/10.1016/j.cub.2016.03.076

Love, M., Anders, S., & Huber, W. (2014). Differential analysis of count data–the DESeq2 package. *Genome Biology*, *15*(550), 1–54.

Maan, M. E., & Cummings, M. E. (2008). Female preferences for aposematic signal components in a polymorphic poison frog. *Evolution*, *62*(9), 2334–2345. https://doi.org/10.1111/j.1558-5646.2008.00454.x

Maan, M. E., & Cummings, M. E. (2009). Sexual dimorphism and directional sexual selection on aposematic signals in a poison frog. *Proceedings of the National Academy of Sciences*, *106*(45), 19072–19077. https://doi.org/10.1073/pnas.0903327106

Maan, M. E., & Cummings, M. E. (2012). Poison frog colors are honest signals of toxicity, particularly for bird predators. *The American Naturalist*, *179*(1), E1–E14. https://doi.org/10.1086/663197

Mallet, J., & Barton, N. H. (1989). Strong natural selection in a warning-color hybrid zone. *Evolution*, 421–431. https://doi.org/10.1111/j.1558-5646.1989.tb04237.x

Mamrot, J., Legaie, R., Ellery, S. J., Wilson, T., Seemann, T., Powell, D. R., … Dickinson, H. (2017). De novo transcriptome assembly for the spiny mouse (*Acomys cahirinus*). *Scientific Reports*, *7*(1), https://doi.org/10.1038/s41598-017-09334-7

Marill, J., Capron, C. C., Idres, N., & Chabot, G. G. (2002). Human cytochrome P450s involved in the metabolism of 9-cis- and 13-cis-retinoic acids. *Biochemical Pharmacology*, *63*(5), 933–943. https://doi.org/10.1016/S0006-2952(01)00925-X

Marill, J., Cresteil, T., Lanotte, M., & Chabot, G. G. (2000). Identification of human cytochrome P450s involved in the formation of all-trans-retinoic acid principal metabolites. *Molecular Pharmacology*, *58*(6), 1341–1348. https://doi.org/10.1124/mol.58.6.1341

Martini, R., & Murray, M. (1993). Participation of P450 3A enzymes in rat hepatic microsomal retinoic acid 4-hydroxylation. *Archives of Biochemistry and Biophysics*, *303*(1), 57–66. https://doi.org/10.1006/abbi.1993.1255

Mast, N., White, M. A., Bjorkhem, I., Johnson, E. F., Stout, C. D., & Pikuleva, I. A. (2008). Crystal structures of substrate-bound and substrate-free cytochrome P450 46A1, the principal cholesterol hydroxylase in the brain. *Proceedings of the National Academy of Sciences*, *105*(28), 9546–9551. https://doi.org/10.1073/pnas.0803717105

Matsui, K., Marunouchi, J., & Nakamura, M. (2002). An ultrastructural and carotenoid analysis of the red ventrum of the Japanese newt, *Cynops pyrrhogaster*. *Pigment Cell Research*, *15*(4), 265–272. https://doi.org/10.1034/j.1600-0749.2002.01085.x

McGraw, K. J. (2006). Mechanics of carotenoid-based coloration. In G. E. Hill & K. J. McGraw (Eds.), *Bird Coloration: Mechanisms and measurements* (pp. 177–242). Cambridge, MA: Harvard University Press.

McKinnon, J. S., & Pierotti, M. E. R. (2010). Colour polymorphism and correlated characters: Genetic mechanisms and evolution. *Molecular Ecology*, *19*(23), 5101–5125. https://doi.org/10.1111/j.1365-294X.2010.04846.x

McLean, C. A., Lutz, A., Rankin, K. J., Stuart-Fox, D., & Moussalli, A. (2017). Revealing the biochemical and genetic basis of color variation in a polymorphic lizard. *Molecular Biology and Evolution*, *34*(8), 1924–1935. https://doi.org/10.1093/molbev/msx136

McLean, C. A., & Stuart-Fox, D. (2014). Geographic variation in animal colour polymorphisms and its role in speciation. *Biological Reviews*, *89*(4), 860–873. https://doi.org/10.1111/brv.12083

Mundy, N. I., Stapley, J., Bennison, C., Tucker, R., Twyman, H., Kim, K.-W., … Slate, J. (2016). Red carotenoid coloration in the Zebra Finch is controlled by a cytochrome P450 gene cluster. *Current Biology*, *26*(11), 1435–1440. https://doi.org/10.1016/j.cub.2016.04.047

Nguyen, L.-T., Schmidt, H. A., von Haeseler, A., & Minh, B. Q. (2014). IQ-TREE: A fast and effective stochastic algorithm for estimating maximum-likelihood phylogenies. *Molecular Biology and Evolution*, *32*(1), 268–274. https://doi.org/10.1093/molbev/msu300

Obika, M., & Bagnara, J. T. (1964). Pteridines as pigments in amphibians. *Science*, *143*(3605), 485–487. https://doi.org/10.1126/science.143.3605.485

Ojima, K., Breitenbach, J., Visser, H., Setoguchi, Y., Tabata, K., Hoshino, T., … Sandmann, G. (2006). Cloning of the astaxanthin synthase gene from *Xanthophyllomyces dendrorhous* (*Phaffia rhodozyma*) and its assignment as a β-carotene 3-hydroxylase/4-ketolase. *Molecular Genetics and Genomics*, *275*(2), 148–158. https://doi.org/10.1007/s00438-005-0072-x

Palczewski, G., Amengual, J., Hoppel, C. L., & von Lintig, J. (2014). Evidence for compartmentalization of mammalian carotenoid metabolism. *The FASEB Journal*, *28*(10), 4457–4469. https://doi.org/10.1096/fj.14-252411

Rambaut, A. (2014). *FigTree 1.4. 2 software*. Edinburgh: Institute of Evolutionary Biology, Univ.

Rendic, S., & Guengerich, F. P. (2015). Survey of human oxidoreductases and cytochrome P450 enzymes involved in the metabolism of xenobiotic and natural chemicals. *Chemical Research in Toxicology*, *28*(1), 38–42. https://doi.org/10.1021/tx500444e

Richards-Zawacki, C. L., Wang, I. J., & Summers, K. (2012). Mate choice and the genetic basis for colour variation in a polymorphic dart frog: Inferences from a wild pedigree. *Molecular Ecology*, *21*(15), 3879–3892. https://doi.org/10.1111/j.1365-294X.2012.05644.x

Rodriguez-Amaya, D. B. (2001). *A guide to carotenoid analysis in foods*. Washington, DC: ILSI Press.

Santos, J. C., Coloma, L. A., & Cannatella, D. C. (2003). Multiple, recurring origins of aposematism and diet specialization in poison frogs. *Proceedings of the National Academy of Sciences*, *100*(22), 12792–12797. https://doi.org/10.1073/pnas.2133521100

Saporito, R. A., Donnelly, M. A., Spande, T. F., & Garraffo, H. M. (2012). A review of chemical ecology in poison frogs. *Chemoecology*, *22*(3), 159–168. https://doi.org/10.1007/s00049-011-0088-0

Stuckert, A. M. M., Moore, E., Coyle, K. P., Davison, I., MacManes, M. D., Roberts, R., & Summers, K. (2019). Variation in pigmentation gene expression is associated with distinct aposematic color morphs in the poison frog *Dendrobates auratus*. *BMC Evolutionary Biology*, *19*(1), 85. https://doi.org/10.1186/s12862-019-1410-7

Summers, K., & Clough, M. E. (2001). The evolution of coloration and toxicity in the poison frog family (Dendrobatidae). *Proceedings of the National Academy of Sciences*, *98*(11), 6227–6232. https://doi.org/10.1073/pnas.101134898

Summers, K., Symula, R., Clough, M., & Cronin, T. (1999). Visual mate choice in poison frogs. *Proceedings of the Royal Society of London. Series B: Biological Sciences*, *266*(1434), 2141–2145. https://doi.org/10.1098/rspb.1999.0900

Symula, R., Schulte, R., & Summers, K. (2001). Molecular phylogenetic evidence for a mimetic radiation in Peruvian poison frogs supports a Müllerian mimicry hypothesis. *Proceedings of the Royal Society of London. Series B: Biological Sciences*, *268*(1484), 2415–2421.

Toews, D. P. L., Hofmeister, N. R., & Taylor, S. A. (2017). The evolution and genetics of carotenoid processing in animals. *Trends in Genetics*, *33*(3), 171–182. https://doi.org/10.1016/j.tig.2017.01.002

Twomey, E., Johnson, J. D., Castroviejo-Fisher, S., & Van Bocxlaer, I. (2020). Data from: A ketocarotenoid-based color polymorphism in the Sira poison frog *Ranitomeya sirensis* indicates novel gene interactions underlying aposematic signal variation. *Molecular Ecology*, *Dryad Digital Repository*. https://doi.org/10.5061/dryad.wpzgmsbj2

Twomey, E., Kain, M., Claeys, M., Summers, K., Castroviejo-Fisher, S., & Van Bocxlaer, I. (2020). Mechanisms for color convergence in a mimetic radiation of poison frogs. *The American Naturalist*, *195*(5), E132–E149. https://doi.org/10.1086/708157

Twomey, E., Vestergaard, J. S., & Summers, K. (2014). Reproductive isolation related to mimetic divergence in the poison frog *Ranitomeya imitator*. *Nature Communications*, *5*(4749), 1–8.

Twomey, E., Vestergaard, J. S., Venegas, P. J., & Summers, K. (2015). Mimetic divergence and the speciation continuum in the mimic poison frog *Ranitomeya imitator*. *The American Naturalist*, *187*(2), 205–224. https://doi.org/10.1086/684439

Twyman, H., Prager, M., Mundy, N. I., & Andersson, S. (2018). Expression of a carotenoid-modifying gene and evolution of red coloration in weaverbirds (Ploceidae). *Molecular Ecology*, *27*(2), 449–458. https://doi.org/10.1111/mec.14451

Twyman, H., Valenzuela, N., Literman, R., Andersson, S., & Mundy, N. I. (2016). Seeing red to being red: Conserved genetic mechanism for red cone oil droplets and co-option for red coloration in birds and turtles. *Proceedings of the Royal Society B: Biological Sciences*, *283*(1836), 20161208. https://doi.org/10.1098/rspb.2016.1208

Veerman, A. (1970). The pigments of Tetranychus cinnabarinus boisd. (Acari: Tetranychidae). *Comparative Biochemistry and Physiology*, *36*(4), 749–763. https://doi.org/10.1016/0010-406X(70)90530-X

Verleun, T. (2018). Ranitomeya perikelen. *Dendrobatidae Nederland Magazine*, *3*, 26–30.

von Lintig, J. (2010). Colors with functions: Elucidating the biochemical and molecular basis of carotenoid metabolism. *Annual Review of Nutrition*, *30*(1), 35–56. https://doi.org/10.1146/annurev-nutr-080508-141027

Wang, I. J., & Summers, K. (2010). Genetic structure is correlated with phenotypic divergence rather than geographic isolation in the highly polymorphic strawberry poison-dart frog. *Molecular Ecology*, *19*(3), 447–458. https://doi.org/10.1111/j.1365-294X.2009.04465.x

Weaver, R. J., Cobine, P. A., & Hill, G. E. (2018). On the bioconversion of dietary carotenoids to astaxanthin in the marine copepod, *Tigriopus californicus*. *Journal of Plankton Research*, *40*(2), 142–150. https://doi.org/10.1093/plankt/fbx072

Weaver, R. J., Santos, E. S. A., Tucker, A. M., Wilson, A. E., & Hill, G. E. (2018). Carotenoid metabolism strengthens the link between feather coloration and individual quality. *Nature Communications*, *9*(1), 1–9. https://doi.org/10.1038/s41467-017-02649-z

Wybouw, N., Kurlovs, A. H., Greenhalgh, R., Bryon, A., Kosterlitz, O., Manabe, Y., … Van Leeuwen, T. (2019). Convergent evolution of cytochrome P450s underlies independent origins of keto-carotenoid pigmentation in animals. *Proceedings of the Royal Society B: Biological Sciences*, *286*(1907), 20191039. https://doi.org/10.1098/rspb.2019.1039

Yang, Y., Blomenkamp, S., Dugas, M. B., Richards-Zawacki, C. L., & Pröhl, H. (2019). Mate choice versus mate preference: Inferences about color-assortative mating differ between field and lab assays of poison frog behavior. *The American Naturalist*, *193*(4), 598–607. https://doi.org/10.1086/702249

SUPPORTING INFORMATION

Additional supporting information may be found online in the Supporting Information section.

How to cite this article: Twomey E, Johnson JD, Castroviejo-Fisher S, Van Bocxlaer I. A ketocarotenoid-based colour polymorphism in the Sira poison frog *Ranitomeya sirensis* indicates novel gene interactions underlying aposematic signal variation. *Mol Ecol*. 2020;29:2004–2015. https://doi.org/10.1111/mec.15466